

Friction and wear studies of octadecyltrichlorosilane SAM on silicon

Sili Ren^{a,b}, Shengrong Yang^{a*}, Yapu Zhao^b, Jinfang Zhou^a, Tao Xu^a and Weimin Liu^a

^aState Key Laboratory of Solid Lubrication, Lanzhou Institute of Chemical Physics, Chinese Academy of Sciences, Lanzhou 730000, China

^bState Key Laboratory of Nonlinear Mechanics, Institute of Mechanics, Chinese Academy of Sciences, Beijing 100080, China

Received April 7, 2002; accepted June 30, 2002

A self-assembled monolayer of octadecyltrichlorosilane (OTS) was prepared on a single-crystal silicon wafer (111) and its tribological properties were examined with a one-way reciprocating tribometer. The worn surfaces and transfer film on the counterface were analyzed by means of scanning electron microscopy and X-ray photoelectron spectroscopy. The results show that, due to the wear of the OTS monolayer and the formation of the transfer film on the counterpart ball, the friction coefficient gradually increases from 0.06 to 0.13 with increasing sliding cycles and then keeps stable at a normal load of 0.5 N. The transfer film is characterized by deposition, accumulation, and spalling at extended test duration. Though low friction coefficients of the monolayer in sliding against steel or ceramic counterfaces are recorded, poor load-carrying capacity and antiwear ability are also shown. Moreover, the monolayer itself or the corresponding transfer film on the counterface fails to lubricate even at a normal load of 1.0 N. Thus, the self-assembled monolayer of octadecyltrichlorosilane can be a potential boundary lubricant only at very low loads.

KEY WORDS: self-assembled monolayer; tribological properties; transfer film; OTS

1. Introduction

Micro-miniaturization is a current trend in the development of many electrical devices, especially the electromechanical ones, known as the microelectromechanical systems (MEMS) [1], which possess superior performance and low unit cost. However, the large surface-area-to-volume ratios of planar, bulk, and LIGA-processed micromechanisms bring the problem of adhesion into the MEMS [2]. In these systems, contact and separation between the component surfaces often repeatedly occur in the very small contact areas where adhesion and friction forces may predominate over inertial and gravitational forces to dominate the performance of the devices [3,4]. Owing to the microsize of the MEMS components, conventional lubricants are no longer the most desirable ones.

Self-assembled monolayers (SAMs), a preferred kind of boundary lubricant, which are formed spontaneously in a simple way by immersing an appropriate substrate into a solution of active surfactant in an organic solvent [5], have witnessed tremendous growth in the nano-tribological field in the past 15 years [6–10]. Two kinds of SAMs, namely, the monolayers of alkanethiolates on gold surfaces and monolayers of organosilicon derivatives on silicon or mica wafer surfaces, have attracted much attention because of their excellent tribological properties. Since silicon has been the most widely used material in MEMS [11], the latter may have the largest potential in the application of lubrications for MEMS.

Srinivasan and co-workers [2] investigated the stiction of two types of SAMs derived from the precursor molecules of octadecyltrichlorosilane ($\text{CH}_3(\text{CH}_2)_{17}\text{SiCl}_3$, coded as OTS) and (1H, 1H, 2H, 2H)-perfluorooctadecyltrichlorosilane ($\text{CF}_3(\text{CF}_2)_7(\text{CH}_2)_2\text{SiCl}_3$, coded as FOTS) which were used as boundary lubricants in polycrystalline silicon microstructures. They found that the release-related stiction associated with water capillary forces was eliminated due to the hydrophobicity of these SAMs, and the in-use stiction was also greatly reduced. Adhesive experiments demonstrated that SAM of OTS reduced adhesion by more than threefold over the conventional process and that the fluorinated SAMs can lessen it further by four times. The effects of pH on adhesion and friction forces between SAM of alkylsilanes with various terminal groups (CH_3 , NH_2 , and SO_3H) in aqueous solutions and the tribological behavior of OTS monolayers in the solvent environment were focused on as well [12,13]. However, few systematic studies have been concerned with the wear resistance and direct proofs of the wear of the OTS monolayer and the formation of the transfer film on the counterface.

This paper deals with the friction and wear behavior of the SAM of OTS on a single-crystal silicon surface, with emphasis on wear and confirmation of the transfer of the OTS monolayer.

2. Experimental

2.1. Materials

Polished single-crystal silicon (111) wafers (obtained from GRINM Semiconductor Materials Co., Ltd.,

* To whom correspondence should be addressed.
E-mail: sryang@ns.lzb.ac.cn

Beijing) with a roughness of about 0.4 nm after cleaning were used as the substrate. Chemical reagent $\text{CH}_3(\text{CH}_2)_{17}\text{SiCl}_3$ (90%) provided by Aldrich without further purification was used for the preparation of the SAM. Toluene (99.5%, anhydrous), absolute ethanol (99.8%) and ultra-pure water with resistivity of $18.3\text{ M}\Omega$ were also used for the preparation of the monolayer.

2.2. Preparation of the SAM of OTS

Silicon wafers were cleaned and hydroxylated by immersing in a piranha solution (a mixture of 7:3 (V/V) 98% H_2SO_4 and 30% H_2O_2) at 90°C for 30 min. The wafers were then rinsed with adequate ultra-pure water five times and dried by nitrogen blowing. The cleaned substrates were placed into the OTS solution of concentration of $3.0 \times 10^{-3}\text{ M}$ in toluene and held for 6 h. Then the functionalized substrates were washed sequentially with toluene and ethanol to eliminate any possible physisorbed impurities.

2.3. Characterization of the SAM of OTS

The static contact angles for ultra-pure water on the SAM were measured with a Kyowa contact-angle meter. At least three replicate measurements were carried out for each specimen, and the error was below 2. The contact angle for ultra-pure water on the OTS monolayer was about 112° , which agreed well with that reported [2,13].

The thickness of the monolayer was measured on a Gaertner L116-E ellipsometer, which was equipped with a He-Ne laser (632.8 nm) set at an incident angle of 70° . A real refractive index of 1.429 was assumed for the SAM of OTS. Three or four replicate measurements were carried out for each specimen and the thickness was recorded to an accuracy of $\pm 0.3\text{ nm}$. The thickness of the silicon oxides and OTS monolayer was about 2.0 nm and 2.6 nm, respectively, which was also consistent with the reported values [13].

Fourier transform infrared spectra of the SAM of OTS were recorded on an IFS66V Fourier Transform Infrared Spectrometer with a resolution of 4 cm^{-1} , using transmission mode.

An atomic force microscope of model SPA400 (Seiko Instruments Inc.) was used to observe the morphology of the SAM of OTS, using the "Tapping Scanning" mode to obtain the morphology image.

2.4. Tribological behavior

Friction and wear tests were carried out on a DF-PM one-way reciprocating tribometer. Details of the tribometer are available elsewhere [14]. The lower specimen of silicon wafer with SAM film slides for a distance

of 7 mm under selected normal load applied to the stationary ball by an arm attached to a dead weight, then it stops at the end of each sliding pass and keeps off contact with the upper ball and returns to the original starting position, followed by the same repetitive procedures. Two kinds of counterpart ball ($\phi 4\text{ mm}$) were used. One was made of AISI-52100 steel (mass composition 0.95–1.05% C, 1.30–1.65% Cr, 0.15–0.35% Si, 0.20–0.40% Mn, $<0.027\%$ P, $<0.020\%$ S, $<0.30\%$ Ni, $<0.25\%$ Cu, balance Fe, HRc59-61). The other was made of Si_3N_4 . Prior to the friction and wear test, the ceramic or steel ball was cleaned with acetone-soaked cotton. Loads of 0.05, 0.5, and 1 N were selected and the corresponding initial Hertzian contact stresses were about 0.3, 0.7, and 0.9 GPa, respectively. Sliding velocity was about 90 mm/min. All the tests were conducted at room temperature and a relative humidity of 45%. The friction coefficient and sliding cycles were recorded automatically. It was assumed that lubrication failure of the ultra-thin film occurred as the friction coefficient rose sharply to a higher and stable value similar to that of a cleaned silicon oxide wafer against the same counterface (about 0.65). The number of sliding cycles at this point was recorded as the wear life of the ultra-thin film.

The chemical states of the typical elements on the worn surface of the counterpart steel were examined with a PHI-5702 multi-functional X-ray photoelectron spectrometer (XPS), using a pass energy of 29.35 eV and an excitation source of Mg- $\text{K}\alpha$ radiation ($h\nu=1253.6\text{ eV}$). The binding energy of contaminated carbon (C_{1s} : 284.6 eV) was used as the reference. The morphologies of the wear scar of the ultra-thin film and the counterpart steel balls were observed with a JSM-5600LV scanning electron microscope (SEM).

3. Results and discussion

3.1. Structure and morphology characterization

The transmission infrared spectrum of the SAM of OTS on silicon wafer in the frequency range of $3000\text{--}2800\text{ cm}^{-1}$ is shown in figure 1. For comparison, the spectrum of an isotropic bulk sample of OTS is also presented. It can be seen that the peak frequencies for asymmetric and symmetric methylene vibrations, $\nu_{\text{as}}(\text{CH}_2)$ and $\nu_{\text{s}}(\text{CH}_2)$, shift to lower values for the ultra-thin film of OTS. Namely, the peak frequencies $\nu_{\text{as}}(\text{CH}_2)$ and $\nu_{\text{s}}(\text{CH}_2)$ for the isotropic bulk sample of OTS shift from 2923 and 2853 cm^{-1} , respectively, to 2918 and 2850 cm^{-1} , respectively, for the SAM of OTS. Such a shift suggests that the SAM of OTS is in a highly ordered or crystallized state [15].

Figure 2 shows the AFM morphological images of the cleaned silicon wafer and the SAM of OTS. Some holes and grains are seen on the surface of silicon wafer (figure 2(a)), which could be caused by the intensive

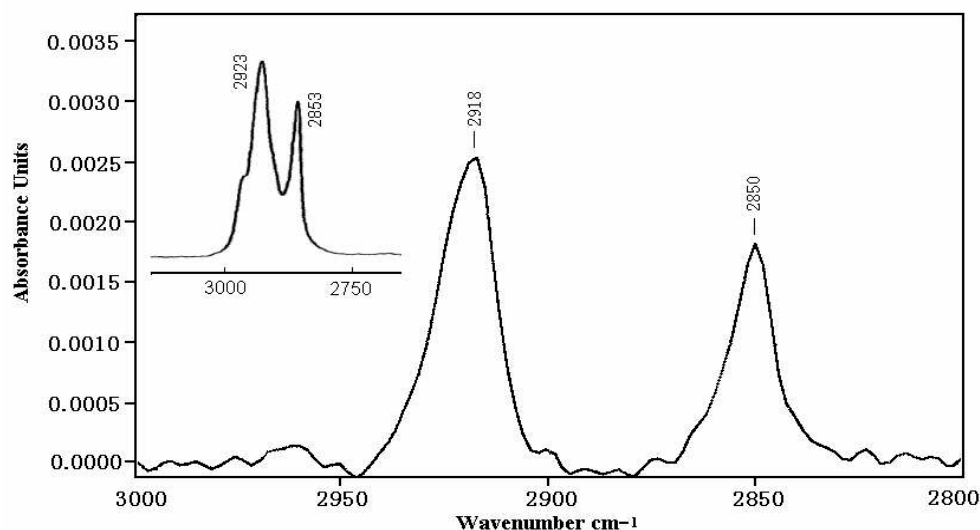


Figure 1. Transmission IR spectra of the SAM of OTS on silicon wafer in the high-frequency region. The spectrum of an isotropic bulk sample of OTS is also presented in the top left corner for comparison.

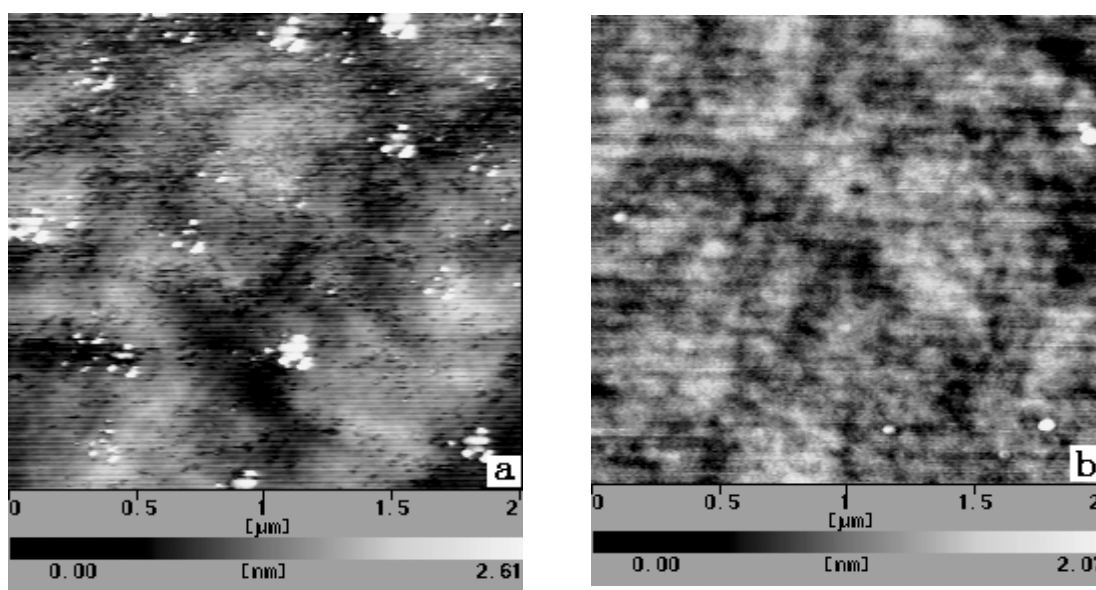


Figure 2. AFM topographic images of the silicon wafer (a) and the SAM of OTS on the silicon wafer (b).

erosion of Piranha solution to the silicon wafer. After deposition of the ultra-thin film of OTS on the silicon wafer substrate, the holes disappear and only a few grains are visible (figure 2(b)). The root-mean-square (rms) micro-roughness of the monolayer is estimated to be 0.3 nm over an area of $2 \times 2 \mu\text{m}$, which is a little bit lower than that of the silicon wafer substrate surface (rms 0.4 nm). These observations indicate that the SAM of OTS on the silicon wafer is quite smooth and homogenous. Accordingly, it can be inferred that the incorporation of the SAM of OTS helps to improve the surface qualities of the silicon wafer substrate.

3.2. Friction and wear behavior

Figure 3 shows the variation in the friction coefficients with sliding cycles in the sliding of the OTS monolayer against the Si_3N_4 ball at a normal load of 0.5 N and a sliding velocity of 90 mm/min. It can be seen that the initial coefficient is as low as 0.06. Such a lower friction coefficient might attributed to the fact that SAMs are ordered molecular assemblies in which one end of the long-chain molecules is attached to the substrate surface [5]. The alkyl chains may thus have a significant freedom of swing and rearrange along the

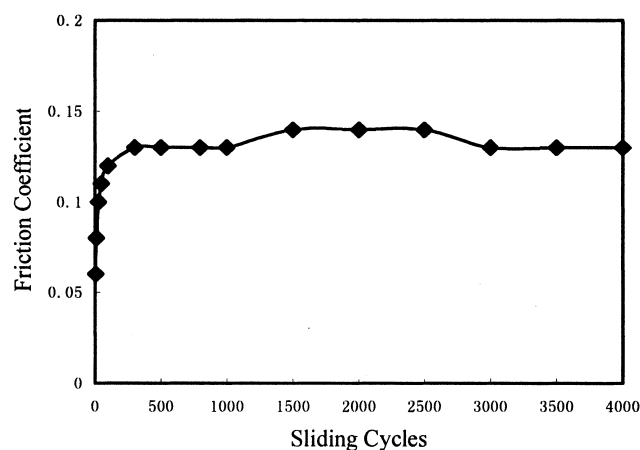


Figure 3. Variation in the friction coefficients with sliding cycles for the SAM of OTS sliding against a Si_3N_4 ball at a normal load of 0.5 N and a sliding velocity of 90 mm/min.

sliding direction under shear stress [16], and therefore yield a smaller resistance. In addition, the lower surface energy of the SAM might be another important reason for the lower friction. However, it should be pointed out that the low friction coefficient 0.06 tested in our work is much higher than what was reported for the same film on microscopic testing with AFM/FFM (0.018) [17]. Such a difference can be attributed to the considerably different sliding velocities and surface morphologies of the sliders.

More detailed information can be obtained from figure 3, in which the friction coefficient rises to a stable and slightly high value (0.13×0.14) after experiencing the low value (0.06). This indicates that wear of the OTS monolayer occurred. Nonetheless, a low friction coefficient of about 0.13×0.14 was still registered in the sliding of the monolayer against the Si_3N_4 ball even at an extended sliding cycle of 4000. This implies that the counterpart ceramic ball was modified by the worn and transferred OTS during sliding, and both the worn monolayer itself and the transfer film co-worked as boundary lubricants.

In order to find the evidence for the above-mentioned modification of the counterpart ceramic ball by the worn and transferred OTS material, we investigated the friction behavior of bare silicon wafer sliding against modified and unmodified counterpart Si_3N_4 balls at a normal load of 0.05 N (the modified Si_3N_4 ball was obtained by sliding the SAM of OTS against it for 800 cycles). The results are shown in figure 4. It can be seen that the friction coefficient of the bare silicon wafer sliding against the modified Si_3N_4 ball is about 0.24, which is significantly smaller than that against the unmodified Si_3N_4 ball. This indicates that the SAM of OTS is liable to be transferred onto the counterface to form a transfer film, and thus reduce friction. Accordingly, wear of the SAM of OTS should be expected if one takes into account such a transfer of the

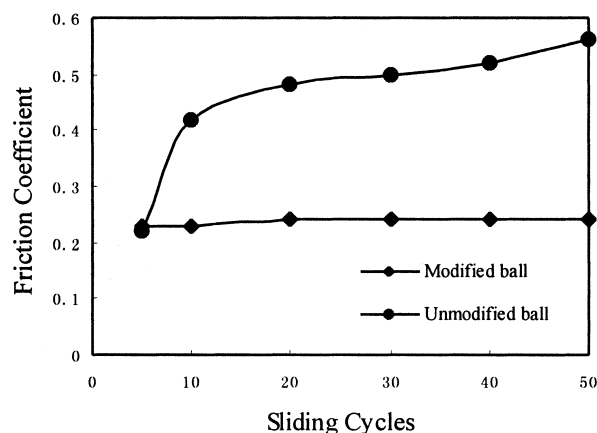
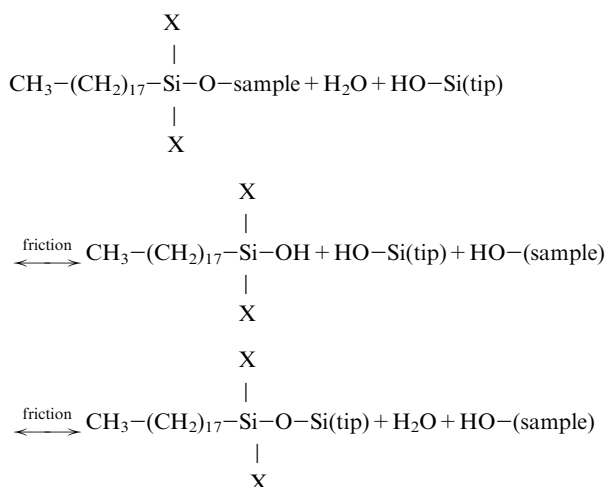


Figure 4. Variation in the friction coefficients with sliding cycles for the bare silicon wafer sliding against modified and unmodified Si_3N_4 balls at a normal load of 0.05 N and a sliding velocity of 90 mm/min.

monolayer onto the counterface. Patton *et al.* [18] studied the effect of humidity on tribological properties of OTS-coated and uncoated motors. They found that uncoated motors exhibited negligible wear and low adhesion only at around 50% RH, and the OTS monolayer could broaden the operating envelope to 30–50% RH. However, they also found that the OTS monolayer could be easily worn at lower (such as 0.1% RH) or high (such as 90% RH) humidity.

In a previous study, DePalma and Tillman [19] also observed that the friction coefficient rose from a lower initial value to a higher value after several sliding cycles during the OTS monolayer sliding against a slider counterface. However, they just attributed such behavior to the baseline drift of the tribometer and then concluded that no wear occurred for the OTS monolayer. Xiao *et al.* [20] reported that the Si_3N_4 tip of the AFM could be modified when it was used to scan the SAM of *n*-octadecyltrimethoxysilane (OTE) on mica. They suggested that modification of the Si_3N_4 tip could take place only when wear of the monolayer occurred, and the modification process could be described as follows:



In our work, whether this tribo-chemical process occurred or not is uncertain, since the bond mode of OTS on silicon oxide is different from that of OTE on mica [20]. Furthermore, as will be shown below, transfer of the OTS onto the counterpart still occurred when a counterpart steel ball was used.

The effect of normal load on the tribological properties of the SAM of OTS is shown in figure 5. The trend of variation of the friction coefficients with sliding cycles at a load of 0.05 N is similar to that in figure 3. In other words, the monolayer is liable to wear and is transferred onto the counterface even at a load as small as 0.05 N. At a relatively high load of 1 N, the friction coefficient rises sharply to 0.62 only after sliding for a few cycles, which is the same as in the case of bare silicon substrate sliding against the ceramic counterface. This indicates that the OTS monolayer itself or the corresponding transfer film on the counterface fails to lubricate.

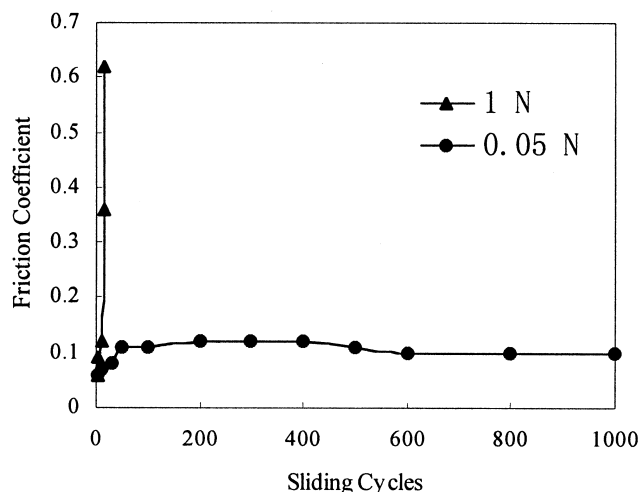


Figure 5. Variation in the friction coefficients with sliding cycles for the SAM of OTS sliding against a Si_3N_4 ball at a sliding velocity of 90 mm/min and normal load of 0.05 N and 1 N, respectively.

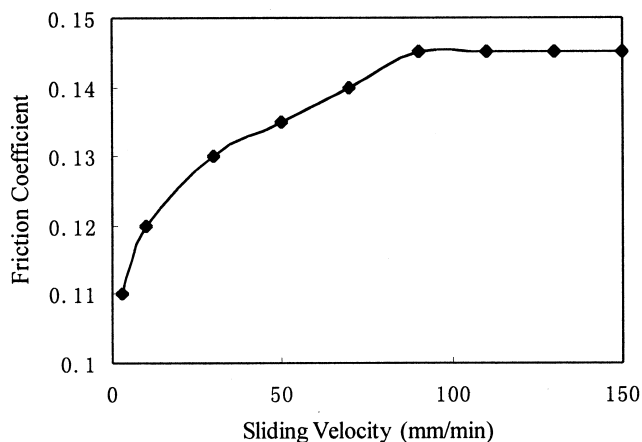


Figure 6. Variation in the friction coefficients with sliding velocities for the SAM of OTS sliding against a Si_3N_4 ball at a normal load of 0.5 N.

These results show that the SAM of OTS has a poor load-carrying capacity and poor antiwear ability. Thus, the OTS monolayer can be a potential lubricant only at very low normal loads.

The effects of sliding velocity on the tribological properties of the OTS monolayer were also studied. Figure 6 shows the variation of the friction coefficient with sliding velocity for the SAM of OTS sliding against a Si_3N_4 ball. The friction coefficient increases steadily

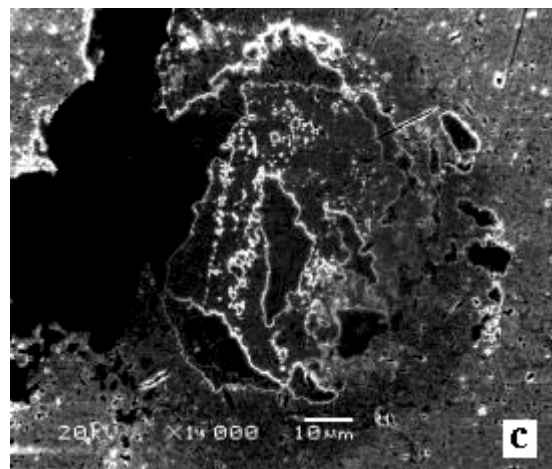
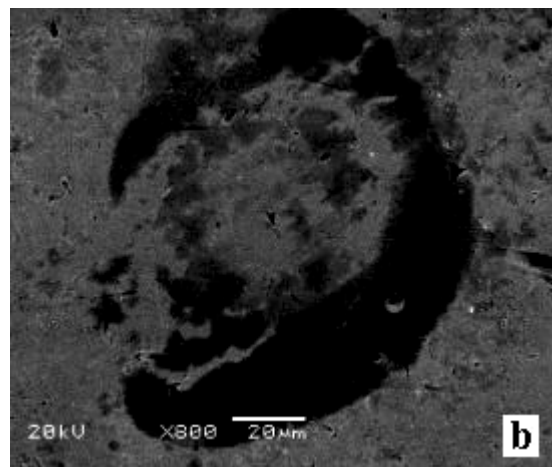
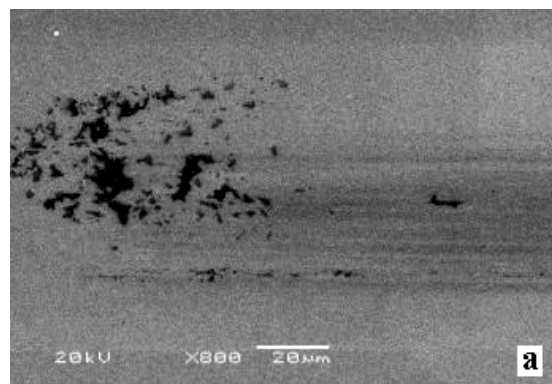


Figure 7. SEM image of the worn surfaces of the SAM of OTS (a), and the counterpart steel ball (b,c).

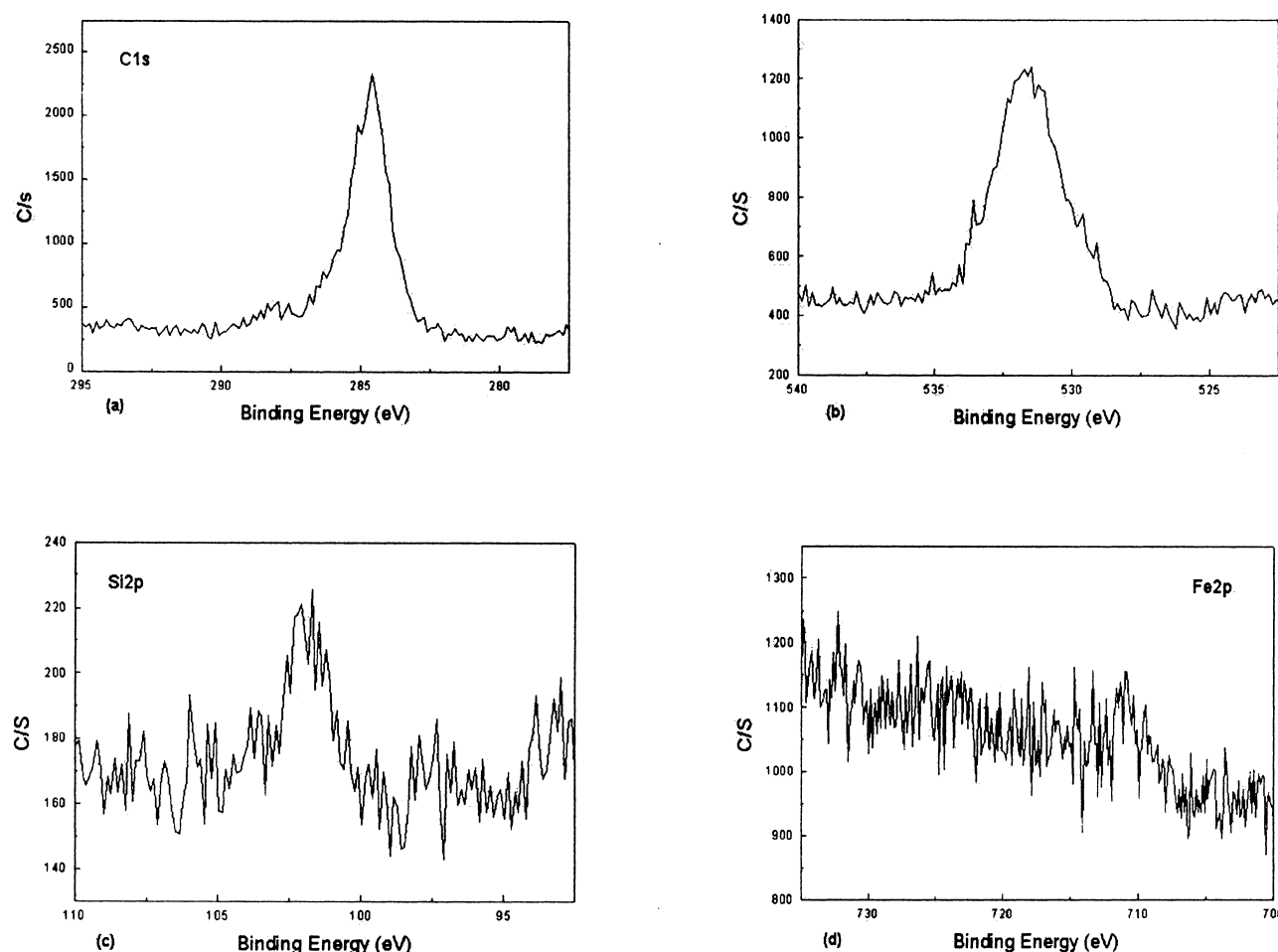


Figure 8. XPS spectra of the transfer film on the wear scar surface of the counterpart steel ball after the SAM of OTS sliding against it for 30 sliding cycles at a normal load of 0.5 N and a sliding velocity of 90 mm/min.

from 0.110 to 0.145 in the range of sliding velocities from 3 to 90 mm/min, and then reaches a plateau for higher velocities. This is in agreement with that reported elsewhere in related microtribological studies [17,21–23] and can be reasonably understood considering the growing dissipation of accumulated energy at higher shear velocities. Liu and co-workers [21] observed that a maximum friction force for self-assembled monolayers of ammonium surfactants on mica appeared at intermediate velocities, which was assumed to be associated with the phase transformation of the monolayer films between “solid” and “liquid” states. Furthermore, they pointed out that the phase transformation of the monolayers was closely related to the chain melting temperatures of the corresponding bulk compounds, in other words, only the compounds whose chain melting temperatures were a little bit higher than room temperature could realize the phase transformation.

3.3. SEM and XPS analyses of the worn surface

The worn surfaces of the SAM of OTS and the corresponding counterpart steel ball were analyzed by means of SEM and XPS. The steel counterpart was selected because it is electrically conductive and hence convenient for the surface analyses. Besides, the SAM of OTS showed similar friction behaviors in sliding against the steel and the ceramic counterparts. It was thus expected that the SEM and XPS analytical results for the steel counterpart ball could be applied to the ceramic counterpart as well. The SEM morphologies of the worn surfaces are given in figure 7. Figure 7(a) shows the worn surfaces of the SAM of OTS after sliding against the steel ball at a load of 0.5 N and a sliding velocity of 90 mm/min for 30 cycles. We can see that the worn surface is characterized by slight scuffing and accumulation of OTS materials at the end of the wear track.

Furthermore, a certain amount of deposits also appear in the wear scar after sliding for 30 cycles (figure 7(b)). This indicates that a significant material transfer occurred and a discontinuous transfer film was formed on the surface of the counterpart steel ball. After sliding for 800 cycles, plate-like wear debris appeared in the wear scar (figure 7(c)), indicating that the transfer film experienced some kind of micro-cracking and spalling at the extended test duration.

Although many difficulties will be encountered when using XPS to characterize the composition of elements on the worn surface (for example, elements of carbon and oxygen could be influenced by environmental dirt), some valuable results are still obtained. Figure 8 shows the binding energies of C_{1s} , O_{1s} , Si_{2p} , and Fe_{2p} on the worn surfaces of steel after sliding against the SAM of OTS at a load of 0.5 N and a sliding velocity of 90 mm/min for 30 cycles. The peak of C_{1s} at 284.6 eV (figure 8(a)) and that of O_{1s} at 531.5 eV (figure 8(b)) can be assigned to C and O elements in the deposits, respectively. Of course, it should be pointed out that both peaks might include the contaminated C and O elements. The peak of Si_{2p} at 101.8 eV (figure 8(c)) is assigned to the Si element in the organic deposits since SiO_2 or Si bristles that might have come from the worn substrate were not observed in the worn scar (figure 7(b)). The appearance of these peaks offers further proof that some of the OTS was really transferred onto the counterpart steel surface and gave birth to a resultant transfer film in sliding against the steel. Furthermore, the Fe_{2p} peak at 710.9 eV has a small intensity (figure 8(d)), indicating that the steel surface is covered or partially covered by the transferred film of the OTS. These SEM and XPS results give a good explanation for the lower friction coefficient in the sliding of silicon wafer against a modified Si_3N_4 ball, as shown in figure 4.

4. Conclusions

Although the SAM of OTS on a silicon wafer experiences wear even at a very early stage of sliding, it still shows a considerably decreased friction coefficient at an extended sliding cycle of 4000. This is attributed to the friction-reduction ability of the ultra-thin film itself and the corresponding deposited or transferred film on the counterpart steel or ceramic surfaces. However, the monolayer of OTS registers poor load-carrying capacity and antiwear

ability in sliding against the steel or ceramic counterface. Moreover, the monolayer itself or the corresponding transfer film on the counterface fails to lubricate even under a normal load of 1.0 N. Therefore, more efforts are needed to develop effective boundary lubricants with improved antiwear ability and load-carrying capacity.

Acknowledgement

The authors wish to acknowledge the financial support of the National Natural Science Foundation of China (Grant No. 50023001), and from CAS (Grant No. KJCX-SW-L2).

References

- [1] V.N. Bliznyuk, M.P. Everson and V.V. Tsukruk, *J. Tribol.* 120 (1998) 489.
- [2] U. Srinivasan, M.R. Houston, R.T. Howe and R. Maboudian, *J. Microelectromechanical Systems* 7 (1998) 252.
- [3] B. Bhushan, A.V. Kulkarni, V.N. Koinkar, M. Boehm, L. Odoni, C. Martelet and M. Belin, *Langmuir* 11 (1995) 3189.
- [4] P.J. Chen and R.J. Wallace, *Vac. Sci. Technol. A.*, 16 (1998) 700.
- [5] A. Ulman, *Chem. Rev.* 96 (1996) 1533.
- [6] S.L. Ren, S.R. Yang, J.Y. Zhang and X.S. Zhang, *Tribol.* 20 (2000) 395 (in Chinese).
- [7] R.W. Carpick and M. Salmeron, *Chem. Rev.* 97 (1997) 1163.
- [8] R. Maboudian and R.T. Howe, *J. Vac. Sci. Technol.* 15 (1997) 1.
- [9] V.N. Bliznyuk, M.P. Everson and V.V. Tsukruk, *ASME J. Trib.* 120 (1998) 489.
- [10] R.R. Rye, G.C. Nelson and M.T. Dugger, *Langmuir* 13 (1997) 2965.
- [11] S.M. Spearing, *Acta. Mater.* 48 (2000) 179.
- [12] V.V. Tsukruk and V.N. Bliznyuk, *Langmuir* 14 (1998) 446.
- [13] S.C. Clear and P.F. Nealey, *Langmuir* 17 (2001) 720.
- [14] L.G. Yu, P.Y. Zhang and Z.L. Du, *Surf. and Coat. Tech.* 130 (2000) 110.
- [15] H.L. Zhang, H. Zhang, J. Zhang, B. Wu, Z.F. Liu and H.L. Li, *Acta Physico-Chimica Sinica* 15 (1999) 657. (in Chinese).
- [16] K.J. Tupper and D.W. Brenner, *Thin Solid Films* 253 (1994) 185.
- [17] V.V. Tsukruk, M.P. Everson, L.M. Lander and W.J. Brittain, *Langmuir* 12 (1996) 3905.
- [18] S.T. Patton, W.D. Cowan, K.C. Eapen and J.S. Zabinski, *Tribol. Lett.* 9 (2001) 199.
- [19] V. DePalma and N. Tillman, *Langmuir* 5 (1989) 868.
- [20] X.D. Xiao, L.M. Qian and S.Z. Wen, *Langmuir* 16 (2000) 662.
- [21] Y.H. Liu, F. Evans, Q. Song and D.W. Grainger, *Langmuir* 12 (1996) 1235.
- [22] S. Gauthier, J.P. Aimé, T. Bouhacina, A.J. Attias and B. Desbat, *Langmuir* 12 (1996) 5126.
- [23] Y.H. Liu, T. Wu and D.F. Evans, *Langmuir* 10 (1994) 2241.